APL Photonics

LETTER | JUNE 01 2020

Injection-seeded backward terahertz-wave parametric oscillator

Yuma Takida ; Kouji Nawata; Hiroaki Minamide

APL Photonics 5, 061301 (2020)
https://doi.org/10.1063/5.0007306

Injection-seeded backward terahertz-wave parametric oscillator

Cite as: APL Photon. 5, 061301 (2020); doi: 10.1063/5.0007306
Submitted: 11 March 2020 • Accepted: 7 May 2020 •
Published Online: 1 June 2020

Yuma Takida,[a] Kouji Nawata, and Hiroaki Minamide

AFFILIATIONS

RIKEN Center for Advanced Photonics, RIKEN, 519-1399 Aramaki-Aoba, Sendai, Miyagi 980-0845, Japan

[a]Author to whom correspondence should be addressed: yuma.takida@riken.jp

ABSTRACT

Engineered quasi-phase-matching in a periodically poled nonlinear crystal has enabled backward optical parametric oscillators, where a pump photon is down-converted to counterpropagating signal and idler photons without an optical cavity. Here, we demonstrate an injection-seeded backward terahertz-wave parametric oscillator (BW-TPO) based on a slant-strip-type periodically poled lithium niobate crystal. A continuous-wave single-frequency laser is used in the BW-TPO pumped by sub-nanosecond 1064.4-nm pulses to provide an injection seed beam for the forward-propagating idler wavelength at 1065.7 nm, resulting in over a 1000-fold enhancement in backward-propagating 0.335-THz output energy, a 63% reduction of the oscillation threshold, and a quantum conversion efficiency as high as 47%. Thanks to the unique advantage of cavity-less oscillation, these improvements and stable operation in the BW-TPO are achieved without any stabilization control of either seed or oscillation modes. Our results show that such an injection-seeded BW-TPO is promising as a compact, efficient, and robust THz-wave source for a wide variety of applications.

Optical parametric oscillators (OPOs) are versatile sources of coherent radiation at the desired wavelength spanning from the near-infrared to the terahertz (THz) region. Conventional OPO configurations rely mainly on two components: (1) a nonlinear optical crystal as a gain medium and (2) an optical cavity as a resonant feedback structure.[1] The latter requires careful alignment and a stabilization system for the robust operation of OPOs as a reliable source not only in fundamental research but also in industrial applications. To address this basic problem, a backward OPO [(BW-OPO), also referred to as a mirrorless OPO] without an optical cavity was proposed by Harris over a half-century ago.[2] While the original BW-OPO considered theoretically was based on birefringence phase matching,[2] its first experimental demonstration was realized using quasi-phase-matching (QPM) in a periodically poled potassium titanyl phosphate (KTP) crystal.[3] However, to satisfy the first-order QPM condition of BW-OPOs operated in the near- or mid-infrared region, challenging fabrication of a very short periodicity less than 1 μm is required to make the grating momentum (k_Λ) sufficiently large.[3–8] In contrast, with a readily available periodicity of several tens of micrometers, we recently demonstrated that it is possible to satisfy the first-order QPM condition for generating backward-propagating frequency-tunable THz waves by using a slant-strip-type periodically poled lithium niobate (PPLN) crystal.[9] Such backward THz-wave parametric oscillators (BW-TPOs) potentially outperform other narrowband THz-wave sources in terms of simplicity and robustness.

In both BW-TPO and BW-OPO processes, the counterpropagating oscillation starts from spontaneous parametric fluorescence and grows in a single-pass interaction through the periodically poled crystal. As a consequence of this cavity-less oscillation, one simple and effective method for reducing the oscillation threshold and improving the conversion efficiency is to implement an optical injection seeding with a continuous-wave (cw) single-frequency laser. Thanks to the unique advantage over conventional cavity-based OPO systems,[10–14] these cavity-less oscillators are free from any complicated controls of spatial and longitudinal mode matching between the seed beam and oscillation mode. Here, we show how cw injection seeding can significantly improve the performance of a sub-nanosecond PPLN BW-TPO.

Figure 1 shows a schematic of the experimental configuration. In this study, we refer to backward- and forward-propagating down-converted waves as THz (signal) and idler, respectively, according

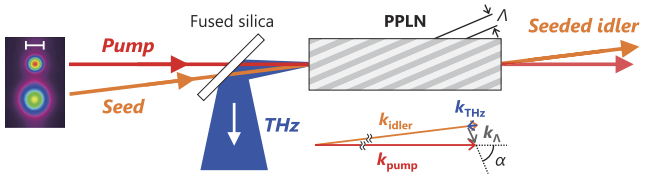

FIG. 1. Experimental configuration. Vector diagram represents the QPM condition of the BW-TPO. The left image shows the spatial profile of the input pump and seed beams measured about 10 cm away from the PPLN crystal. Horizontal scale bar is 1 mm.

to the original BW-OPO proposal.[2] As the gain medium of the BW-TPO, we used a 50 mm-long, 5 mm-wide, 1 mm-thick slant-strip-type PPLN crystal with a poling period of $\Lambda = 53$ μm and a slant angle of $\alpha = 65°$. Both faces of the crystal were coated for anti-reflection (AR) at 1064 nm. The pump source was a laboratory-built Nd:YAG master-oscillator power-amplifier (MOPA) system, providing single-longitudinal-mode, 1064.4 nm, 0.40 ns pulses with up to 5 mJ pulse energy at 100 Hz repetition rate. With this pump wavelength and these PPLN parameters, the first-order QPM of the BW-TPO was calculated to be satisfied to generate backward-propagating THz waves at 0.33 THz and forward-propagating idler at 1065.7 nm at a small quasi-collinear angle of ~0.5° with respect to the pump. For injection seeding of this idler wavelength, the cw output from a fiber-coupled single-frequency laser system (Spectra Quest Lab., Inc.) with a maximum power of 500 mW was used. Both pump and seed beams were collimated and had an FWHM beam diameter of 0.59 mm and 1.0 mm, respectively, as shown by the beam profiles in Fig. 1. To pick the backward-propagating THz wave out of the pump and seed beamlines, a fused silica plate with a 1064-nm AR coating was placed in front of the PPLN crystal with a 45° angle of incidence as a 22% partial reflector at 0.33 THz. The THz-wave signal was then detected using a quasi-optical Schottky-barrier-diode (SBD) receiver with thin-film attenuators or calibrated pyro-electric detector. The forward-propagating idler output separated spatially from the residual pump was measured using an optical energy meter.

Figures 2(a) and 2(b) summarize the THz-wave and idler output energies from the BW-TPO, respectively, as a function of the pump energy with and without a seed beam. With a 480-mW seed power, we observed that BW-TPO oscillation occurred at 1.3 mJ, corresponding to a peak intensity of 1.2 GW/cm^2 for 0.40-ns pump pulses. Above this threshold, the THz-wave output energy increased monotonically and reached 1.5 nJ at the maximum pump energy of 4.5 mJ. The measured oscillation threshold and the THz-wave output at 4.5-mJ pump energy are 63% lower and over 1000-times higher, respectively, than for the unseeded case. Note that the THz-wave output energy reported here was directly measured by the detector with two Tsurupica lenses used for collecting the THz-wave output after reflection at the fused silica plate. By compensating the Fresnel reflection loss of ~44% at the PPLN output face and a partial reflectivity of 22% at the fused silica plate, the THz-wave energy at 4.5-mJ pump energy can be estimated to be 12.2 nJ, corresponding to the pump-to-THz energy conversion efficiency of ~2.7×10^{-6}. Potentially, the extraction efficiency of the fused silica plate could be improved by the implementation of a conductive thin-film coating

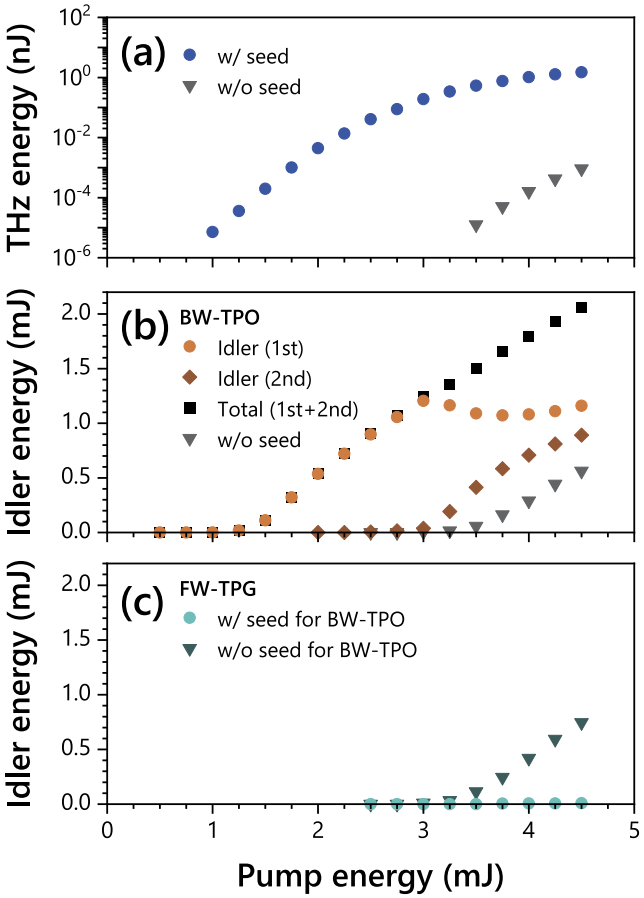

FIG. 2. Injection-seeded BW-TPO output. (a) Backward-propagating THz-wave energy, (b) forward-propagating idler energy, and (c) idler energy from a competitive FW-TPG process as a function of pump energy.

on the surface, such as indium tin oxide (ITO), for high reflectivity at THz frequencies over 90% while keeping the transparency for near-infrared pump and seed beams.

At the pump energy of 3.5 mJ, the wavelength of the backward-propagating THz wave was measured to be 0.894 mm using a scanning Fabry-Pérot etalon consisting of two silicon plates, the result of which is shown in Fig. 3(a). The measured interferometric trace clearly shows a stable single-frequency THz-wave output without any stabilization of the injection seeding. The corresponding frequency of 0.335 THz agreed well with the calculated QPM condition of the BW-TPO. The spectra of the forward-propagating idler were also measured using an optical spectrum analyzer, as shown in Fig. 3(b). While the forward-propagating idler wavelength was observed to be 1065.72 nm, another wavelength peak appeared at 1066.97 nm above the pump energy of 3.0 mJ. This wavelength peak originates from a cascade process of the BW-TPO because the frequency separation of 0.33 THz between the two peaks is in accordance with the backward-propagating THz-wave frequency. The output energy of this cascaded idler is also shown in Fig. 2(b). Including this cascade process, the total idler energy in the

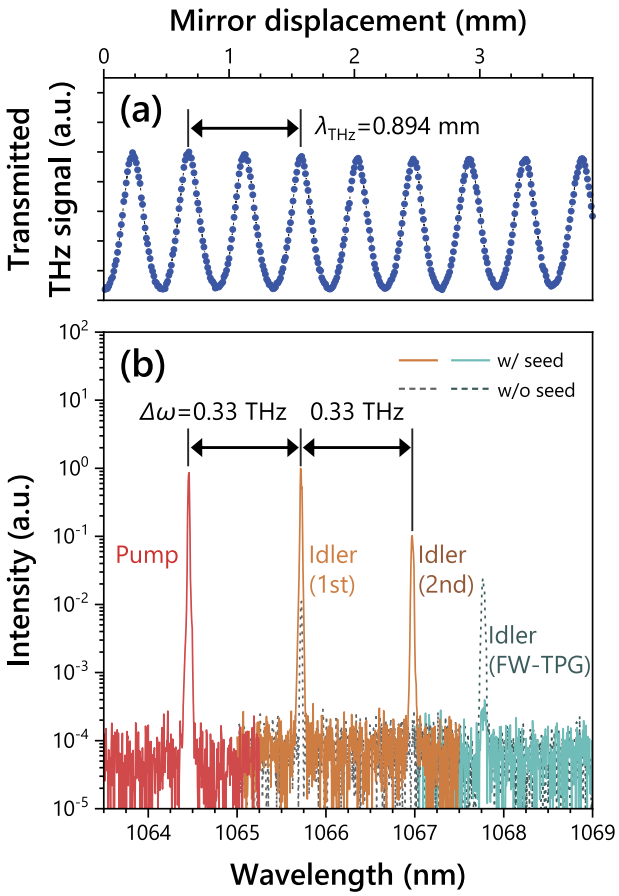

FIG. 3. (a) Measured wavelength of the backward-propagating THz wave. (b) Measured spectra of the pump and idler from both BW-TPO and competitive FW-TPG processes with and without injection seeding for BW-TPO.

injection-seeded BW-TPO was 2.1 mJ at 4.5-mJ pump energy, corresponding to a quantum conversion efficiency of 47%.

From the pump-to-idler quantum conversion efficiency of 47%, the total backward-propagating THz-wave energy generated in the PPLN crystal can be estimated as high as 2.5 μJ with the corresponding pump-to-THz energy conversion efficiency of ~5.6 $\times$ 10^{-4} according to the Manley–Rowe relations. On the other hand, even considering the losses at the PPLN crystal and the fused silica plate, the THz-wave energy observed experimentally was smaller than this estimation by two orders of magnitude. We attributed this discrepancy mainly to the absorption loss for the generated THz waves caused by the room-temperature PPLN crystal. Since the linear absorption coefficient of the PPLN crystal at room temperature is roughly 2.5 cm^{-1} at 0.33 THz,[15,16] the backward-propagating THz-wave energy generated at the center position of the 50 mm-long PPLN crystal suffers from absorption loss before reaching the output face by more than two orders of magnitude. In fact, for cryogenically cooled PPLN crystals with a length of 20 mm or shorter, the enhancement of narrowband THz-wave outputs from optical rectification or difference frequency generation of broadband near-infrared pulses has been reported with pump-to-THz energy conversion efficiencies of up to ~1 $\times$ 10^{-3}.[17,18] Therefore, by decreasing the THz-wave absorption with the cryogenic cooling of the PPLN crystal, a significant improvement to the THz-wave output from the injection-seeded BW-TPO could be achieved toward comparable performances of μJ-level THz-wave output energy and 10^{-3}-order conversion efficiency.

For comparison, idler spectra without injection seeding are also shown by the dashed curves in Fig. 3(b). In this case, idler wavelengths not only from the BW-TPO process at 1065.72 nm but also from another competitive process of forward THz-wave parametric generation (FW-TPG) at 1067.77 nm were observed simultaneously, as reported previously.[9] Both BW-TPO and FW-TPG processes satisfied different QPM conditions in the same PPLN crystal and showed a similar threshold around 3.2-GW/cm^2 peak intensity, as shown in Figs. 2(b) and 2(c). In this experiment, by using injection seeding for the desired process of BW-TPO, we observed that the competitive FW-TPG process can be suppressed by two orders of magnitude, as shown in Figs. 2(c) and 3(b).

For the unseeded BW-TPO process, the oscillation threshold observed in this study was twice as high as the previous result of 1.6 GW/cm^2 with 0.66-ns pump pulses[9] while the same PPLN parameters were employed. The only difference in experimental conditions was that the pump pulse duration was a factor of 1.65 shorter than previously used, resulting in the reduced interaction length of the temporally overlapped counterpropagating pulses inside the PPLN crystal. Optimization of the pump pulse could thus offer an opportunity for further improvement to the BW-TPO threshold and efficiency for both seeded and unseeded cases.

To explore the effect of injection seeding on BW-TPO, we measured the THz-wave and idler outputs as a function of seed power and wavelength. The pump energy was fixed at 2.5 mJ, which was approximately two times higher than the oscillation threshold, not to induce the cascade process, as shown in Fig. 2(b). First, Figs. 4(a) and 4(b) show the measured seed power dependence of THz-wave and idler outputs, respectively. For the seed power above 100 mW, we observed that the THz-wave output continued to grow, but the idler output was saturated. Second, Figs. 4(c) and 4(d) show the measured seed wavelength dependence of THz-wave and idler outputs, respectively, for different seed powers. The wavelength in the cw seed laser was scanned with a 0.5-pm step while keeping the seed beam angle and PPLN conditions. As a result, the acceptance bandwidth at FWHM for the THz wave was measured to be ~0.008 nm, which was nearly independent of seed power. On the other hand, the bandwidth for the idler increased from 0.009 nm to 0.022 nm with the increase in seed power from 1 mW to 400 mW, which is attributed to the saturation behavior as observed in Fig. 4(b). These narrow acceptance bandwidths show the unique property inherent in counterpropagating interaction of cavity-less BW-TPO. In this experiment, we used the collimated pump and seed beams that have flat wavefronts. In the case of an experiment with focused beams, these properties may be affected by changes in wavefront curvature during propagation in the PPLN crystal.

Figures 4(e) and 4(f) show the stability of THz-wave and idler outputs, respectively, at the pump energy of 4.5 mJ with the seed power of 400 mW. Without any stabilization control of mode matching between seed and oscillation modes, the root-mean-square (rms)

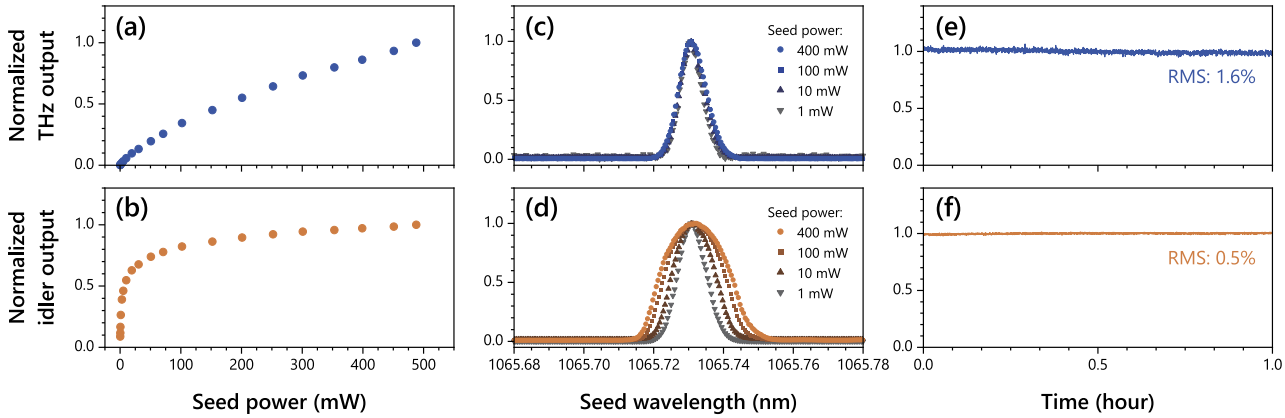

FIG. 4. Normalized backward-propagating THz-wave and forward-propagating idler outputs as a function of seed power [(a) and (b)], seed wavelength [(c) and (d)], and time [(e) and (f)].

fluctuations for 1 h were measured to be 1.6% for the THz wave and 0.5% for the idler. This result represents the key advantage of the simple and robust operation of the injection-seeded BW-TPO, which is essentially important for many applications.

In conclusion, we demonstrated a sub-nanosecond PPLN BW-TPO with cw injection seeding of the forward-propagating idler wavelength. As a result, we achieved over a 1000-fold enhancement in backward-propagating THz-wave output and a 63% reduction of the oscillation threshold compared to the unseeded case. The total quantum conversion efficiency from the pump to the down-converted photons reached as high as 47%. We also note here that the frequency of backward-propagating THz waves in the injection-seeded BW-TPO is continuously tunable by angle tuning of the PPLN crystal in parallel with seed wavelength tuning. We confirmed that a similar performance was obtained within the range of 0.27–0.35 THz. Such an injection-seeded BW-TPO is thus promising as a compact, efficient, and robust THz-wave source for the blooming field of sensing and imaging applications.

This work was supported, in part, by the JSPS KAKENHI (Grant Nos. JP17H01282 and JP18H01906). We thank H. Ito of RIKEN/Tohoku University, M. Kumano of Tohoku University T. Notake of RIKEN, and Y. Tokizane of Tokushima University for helpful discussions. We also thank Y. Higashi, T. Ikeo, Y. Wada, and T. Suzudo of Ricoh Company, Ltd. for the provision of a high-power 808-nm VCSEL module used for the Nd:YAG MOPA pump laser system. We acknowledge the support from the FY2018 RIKEN President's Discretionary Fund.

DATA AVAILABILITY

The data that support the findings of this study are available from the corresponding author upon reasonable request.

REFERENCES

[1]M. H. Dunn and M. Ebrahimzadeh, "Parametric generation of tunable light from continuous-wave to femtosecond pulses," Science **286**, 1513–1517 (1999).
[2]S. E. Harris, "Proposed backward wave oscillation in the infrared," Appl. Phys. Lett. **9**, 114–116 (1966).
[3]C. Canalias and V. Pasiskevicius, "Mirrorless optical parametric oscillator," Nat. Photonics **1**, 459–462 (2007).
[4]G. Strömqvist, V. Pasiskevicius, and C. Canalias, "Self-established noncollinear oscillation and angular tuning in a quasi-phase-matched mirrorless optical parametric oscillator," Appl. Phys. Lett. **98**, 051108 (2011).
[5]C. Liljestrand, A. Zukauskas, V. Pasiskevicius, and C. Canalias, "Highly efficient mirrorless optical parametric oscillator pumped by nanosecond pulses," Opt. Lett. **42**, 2435–2438 (2017).
[6]A. Zukauskas, A.-L. Viotti, C. Liljestrand, V. Pasiskevicius, and C. Canalias, "Cascaded counter-propagating nonlinear interactions in highly-efficient sub-μm periodically poled crystals," Sci. Rep. **7**, 8037 (2017).
[7]R. S. Coetzee, A. Zukauskas, C. Canalias, and V. Pasiskevicius, "Low-threshold, mid-infrared backward-wave parametric oscillator with periodically poled Rb:KTP," APL Photonics **3**, 071302 (2018).
[8]A.-L. Viotti, F. Laurell, A. Zukauskas, C. Canalias, and V. Pasiskevicius, "Coherent phase transfer and pulse compression at 1.4 μm in a backward-wave OPO," Opt. Lett. **44**, 3066–3069 (2019).
[9]K. Nawata, Y. Tokizane, Y. Takida, and H. Minamide, "Tunable backward terahertz-wave parametric oscillation," Sci. Rep. **9**, 726 (2019).
[10]J. E. Bjorkholm and H. G. Danielmeyer, "Frequency control of a pulsed optical parametric oscillator by radiation injection," Appl. Phys. Lett. **15**, 171–173 (1969).
[11]J. M. Boon-Engering, W. E. van der Veer, J. W. Gerritsen, and W. Hogervorst, "Bandwidth studies of an injection-seeded β-barium borate optical parametric oscillator," Opt. Lett. **20**, 380–382 (1995).
[12]K. Imai, K. Kawase, J. Shikata, H. Minamide, and H. Ito, "Injection-seeded terahertz-wave parametric oscillator," Appl. Phys. Lett. **78**, 1026–1028 (2001).
[13]D. Molter, M. Theuer, and R. Beigang, "Nanosecond terahertz optical parametric oscillator with a novel quasi phase matching scheme in lithium niobate," Opt. Express **17**, 6623–6628 (2009).
[14]D. Walsh, D. J. M. Stothard, T. J. Edwards, P. G. Browne, C. F. Rae, and M. H. Dunn, "Injection-seeded intracavity terahertz optical parametric oscillator," J. Opt. Soc. Am. B **26**, 1196–1202 (2009).
[15]L. Pálfalvi, J. Hebling, J. Kuhl, Á. Péter, and K. Polgár, "Temperature dependence of the absorption and refraction of Mg-doped congruent and stoichiometric $LiNbO_3$ in the THz range," J. Appl. Phys. **97**, 123505 (2005).
[16]X. Wu, C. Zhou, W. R. Huang, F. Ahr, and F. X. Kärtner, "Temperature dependent refractive index and absorption coefficient of congruent lithium niobate crystals in the terahertz range," Opt. Express **23**, 29729–29737 (2015).

[17]S. Carbajo, J. Schulte, X. Wu, K. Ravi, D. N. Schimpf, and F. X. Kärtner, "Efficient narrowband terahertz generation in cryogenically cooled periodically poled lithium niobate," Opt. Lett. **40**, 5762–5765 (2015).

[18]F. Ahr, S. W. Jolly, N. H. Matlis, S. Carbajo, T. Kroh, K. Ravi, D. N. Schimpf, J. Schulte, H. Ishizuki, T. Taira, A. R. Maier, and F. X. Kärtner, "Narrowband terahertz generation with chirped-and-delayed laser pulses in periodically poled lithium niobate," Opt. Lett. **42**, 2118–2121 (2017).